DOI: 10.13009/EUCASS2017-228

High Angle of Attack Manoeuvring Control of F-16 Aircraft Based on Nonlinear Dynamic Inversion and Eigenstructure Assignment

Onur ALBOSTAN and Prof. Metin GÖKAŞAN***
**Istanbul Technical University*
Control and Automation Engineering Department, Istanbul Technical University, Istanbul, Turkey
*** Istanbul Technical University*
Control and Automation Engineering Department, Istanbul Technical University, Istanbul, Turkey

Abstract

In this paper, the design of a control law is investigated in order to overcome the high angle of attack manoeuvring control problem. Both linear and nonlinear design methods are analysed with theoretical background. While, linear control laws are synthesized using eigenstructure assignment, the nonlinear control laws are derived by nonlinear dynamic inversion technique. Effectiveness of the proposed control strategies are tested with a high angle of attack manoeuvre on F-16 aircraft model. Superiority of the nonlinear dynamic inversion is demonstrated with graphical results.

1. Introduction

Nonlinear dynamic inversion is the most studied nonlinear control technique for the high angle of attack manoeuvring problem. Nonlinear dynamic inversion is a feedback linearization method which is based on the inversion of the system dynamics [1]. Generally, aircraft dynamics can be separated into two; as slow and fast dynamics and F-16 is not an exception. Slow dynamics are identical for fixed wing aircrafts which can be derived using wind axis differential equations. Fast dynamics on the other hand are unique for each aircraft and aerodynamic database must be included while deriving the fast dynamics of an aircraft.

In this paper, a subsonic aerodynamic database which is based on wind tunnel test results of F-16 at NASA Langley and Ames Research center has been used [1]. This database is valid for $-20° \leq \alpha \leq 90°$, $-30° \leq \beta \leq 30°$ and $V \leq 0.6Mach$ flight conditions. Therefore, it is a suitable platform to test newly developed control laws at high angle of attack region. A 6 DOF mathematical model of F-16 has been developed in Simulink environment. Mathematical model includes aerodynamic database, engine model, atmospheric equations and equations of motion [3], [4]. Trim algorithms for level flight, climb, descend and steady level turning flight conditions have been developed [5]. Furthermore, linearization algorithms have been derived based on the small disturbances theory [6].

In order to compare the performance of nonlinear dynamic inversion control law with a linear control law, linear control augmentation systems for both lateral and longitudinal motion have been designed. Linear control laws were synthesized with eigenstructure assignment technique. Longitudinal controller is a simple angle of attack control command system which is designed using short period dynamics of F-16 aircraft. Lateral controller is a sideslip and stability axis roll-rate command system which is designed using linearized lateral stability axis equations of F-16 aircraft. Design process of linear controllers was finalized with scheduling the gain matrices with respect to altitude and velocity in order to achieve a full-envelope valid flight control law.

Comparison of linear and nonlinear flight control laws was conducted with a predefined high angle of attack manoeuvre. This manoeuvre was defined as a rapid and simultaneous pitch-up and roll motion. While, pull-up motion varies between 20° and 40° of angle of attack, roll motion is kept constant at 120° of bank angle. With increasing values of angle of attack, the longitudinal and lateral dynamics cannot be decoupled, therefore the manoeuvring capability of gain scheduled linear controller and nonlinear dynamic inversion controller becomes significant.

DOI: 10.13009/EUCASS2017-228

2. Nomenclature

S_{ref} : reference wing area $[m^2]$
$\bar{b}$: wing span $[m]$
$\bar{c}$: mean aerodynamic chord $[m]$
Q_c : dynamic pressure $\left[\frac{kg}{ms^2}\right]$
h_{eng} : engine angular momentum $\left[\frac{kg\ m^2}{s}\right]$
I_x, I_y, I_z : moments of inertia $[kg\ m^2]$
I_{xz} : product moment of inertia $[kg\ m^2]$
x_{cg} : center of gravity
x_{cg_r} : reference x_{cg} for aerodynamic data
α : angle of attack $[rad]$
β : angle of sideslip $[rad]$
V_t : true airspeed $[m/s]$
h : pressure altitude $[m]$
g : gravitational acceleration $[m/s^2]$
g_{atm} : atmospheric gravitational acceleration
g_0 : gravitational acceleration at sea level
$a_{x,y,z}$: normal accelerations $[m/s^2]$
A_{x_b,y_b,z_b} : body axis accelerations $[m/s^2]$
ρ : air density $[kg/m^3]$
ρ_0 : air density at sea level
P_0 : air pressure at sea level $[N/m^2]$
δ_{th} : throttle position *(0-1)*
δ_a : aileron deflection $[rad]$
δ_e : elevator deflection $[rad]$
δ_r : rudder deflection $[rad]$
δ_{LEF} : leading edge flap deflection $[rad]$
F_O : body fixed reference frame
F_w : wind axis reference frame
F_S : stability axis reference frame
F_B : body axis reference frame
$\emptyset$: roll angle $[rad]$
θ : pitch angle $[rad]$
ψ : yaw angle $[rad]$
μ : bank angle $[rad]$
γ : flight path angle $[rad]$
χ : heading angle $[rad]$
p, q, r : angular rates $[rad/s]$
R, M, N : body axis moments $[Nm]$
D : drag $[N]$
L : lift $[N]$
Y : side force $[N]$
T : thrust $[N]$
$\bar{X}$: total force at x_b axis $[N]$
$\bar{Y}$: total force at y_b axis $[N]$
$\bar{Z}$: total force at z_b axis $[N]$
$C_{X,Y,Z,l,m,n}$: aerodynamic coefficients

DOI: 10.13009/EUCASS2017-228

3. Nonlinear F-16 Model Description

Aerodynamic model is based on wind tunnel test results of F-16 at NASA Langley and Ames Research center. This database is valid for $-20° \leq \alpha \leq 90°$, $-30° \leq \beta \leq 30°$ and $V_t \leq 0.6\ Mach$ flight conditions
Engine model has been modelled according to the studies [3] and [4]. Engine model data is valid for $V_t \leq 0.6 Mach$ and $h \leq 15240m$ flight conditions.
Control surface actuators are modelled according to the parameters given in Table 1.

Table 1: Actuator Model Parameters

Control	Position Limit	Rate Limit	Time Constant
δ_e	$\pm 25°$	$60d/s$	$0.0495s$
δ_a	$\pm 21.5°$	$80d/s$	$0.0495s$
δ_r	$\pm 30°$	$120d/s$	$0.0495s$
δ_{LEF}	$0{,}25°$	$25d/s$	$0.136s$

Leading edge flap actuator is modelled in an open loop structure. The leading edge flap position is scheduled with angle of attack.

$$\delta_{LEF} = 1.38\left(\frac{2s+7.25}{s+7.25}\right)\alpha - 9.05\left(\frac{1}{2}{V_t}^2\right)\frac{\rho_0}{P_0} + 1.45 \quad \textbf{(1)}$$

Reference frames are demonstrated in Figure 1.

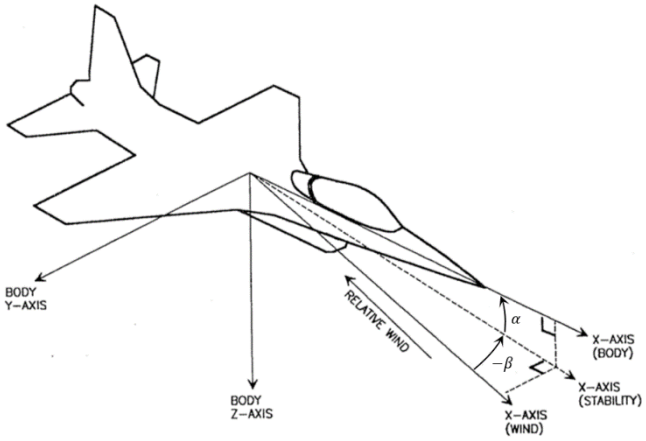

Figure 1: F-16 Reference Frames

Transformation among the reference frames can be stated as follows:

$$F_O \xrightarrow{\chi,\gamma,\mu} F_w \xrightarrow{-\beta} F_S \xrightarrow{\alpha} F_B \quad \leftrightarrow \quad F_O \xrightarrow{\psi,\theta,\phi} F_B$$

where

$$\gamma = sin^{-1}(\cos\alpha\cos\beta\sin\theta - \sin\beta\cos\theta\sin\phi - \sin\alpha\cos\beta\cos\theta\cos\phi) \quad \textbf{(2)}$$

$$\mu = tan^{-1}\left(\frac{\cos\alpha\sin\beta\sin\theta+\cos\beta\cos\theta\sin\phi-\sin\alpha\sin\beta\cos\theta\cos\phi}{\sin\alpha\sin\theta+\cos\alpha\cos\theta\cos\phi}\right) \quad \textbf{(3)}$$

$$\chi = tan^{-1}\left(\frac{\cos\alpha\cos\beta\sin\psi\cos\theta+\sin\beta(\sin\psi\sin\theta\sin\phi+\cos\phi\cos\psi)+\sin\alpha\cos\beta(\sin\psi\sin\theta\cos\phi-\cos\psi\sin\phi)}{\cos\alpha\cos\beta\cos\psi\cos\theta+\sin\beta(\cos\psi\sin\theta\sin\phi-\sin\psi\cos\phi)+\sin\alpha\cos\beta(\cos\psi\sin\theta\cos\phi+\sin\phi\sin\psi)}\right) \quad \textbf{(4)}$$

DOI: 10.13009/EUCASS2017-228

4. Nonlinear Dynamic Inversion

Since there is significant time scale difference between slow and fast dynamics of the F-16 aircraft, nonlinear dynamic inversion method can be applied at two steps [1]. In the first step slow dynamics are inverted to design a controller for α, β, μ inputs and p, q, r outputs. In the second step, fast dynamics are inverted for p, q, r inputs and $\delta_e, \delta_a, \delta_r$ outputs.
Aircraft motion can be expressed in nine state equations:

$$\dot{V}_T = \frac{1}{m}(-D + T\cos\alpha\cos\beta) - g\sin\gamma \tag{5}$$

$$\dot{\alpha} = q - \tan\beta\,(p\cos\alpha + r\sin\alpha) - \frac{1}{mV_T\cos\beta}(L + T\sin\alpha) + \frac{g_{atm}\cos\gamma\cos\mu}{V_T\cos\beta} \tag{6}$$

$$\dot{\beta} = -r\cos\alpha + p\sin\alpha + \frac{1}{mV_T}(Y - T\cos\alpha\sin\beta) + \frac{g_{atm}\cos\gamma\sin\mu}{V_T} \tag{7}$$

$$\dot{\gamma} = \frac{1}{mV_T}[L\cos\mu - Y\sin\mu + T(\cos\alpha\sin\beta\sin\mu + \sin\alpha\cos\mu)] - \frac{g_{atm}}{V_T}\cos\gamma \tag{8}$$

$$\dot{\mu} = \frac{p\cos\alpha + r\sin\beta}{\cos\beta} + \frac{1}{mV_T}[Y\cos\mu\tan\gamma + L(\sin\mu\tan\gamma + \tan\beta) + T(\sin\alpha\tan\gamma\sin\mu + \sin\alpha\tan\beta - \cos\alpha\tan\gamma\cos\mu\sin\beta)] - \frac{g_{atm}\cos\gamma\cos\mu\tan\beta}{V_T} \tag{9}$$

$$\dot{\chi} = \frac{1}{mV_T\cos\gamma}[L\sin\mu + Y\cos\mu + T(\sin\alpha\sin\mu - \cos\alpha\sin\beta\cos\mu)] \tag{10}$$

$$\dot{p} = (c_1 r + c_2 p)\,q + c_3\,R + c_4\big(N + qh_{eng}\big) \tag{11}$$

$$\dot{q} = c_5\,pr - c_6(p^2 - r^2) + c_7\big(M - rh_{eng}\big) \tag{12}$$

$$\dot{r} = (c_8 p - c_2 r)\,q + c_4 R + c_9\big(N + qh_{eng}\big) \tag{13}$$

where

$c_1 = \big((I_{yy} - I_{zz})\cdot I_{zz} - {I_{xz}}^2\big)/\big(I_{xx}\cdot I_{zz} - {I_{xz}}^2\big)$, $c_2 = \big((I_{xx} - I_{yy} + I_{zz})\cdot I_{xz}\big)/\big(I_{xx}\cdot I_{zz} - {I_{xz}}^2\big)$,

$c_3 = I_{zz}/\big(I_{xx}\cdot I_{zz} - {I_{xz}}^2\big)$, $c_4 = I_{xz}/\big(I_{xx}\cdot I_{zz} - {I_{xz}}^2\big)$, $c_5 = (I_{zz} - I_{xx})/I_{yy}$, $c_6 = I_{xz}/I_{yy}$, $c_7 = 1/I_{yy}$,

$c_8 = \big(I_{xx}\cdot(I_{xx} - I_{yy}) + {I_{xz}}^2\big)/\big(I_{xx}\cdot I_{zz} - {I_{xz}}^2\big)$, $c_9 = I_{xx}/\big(I_{xx}\cdot I_{zz} - {I_{xz}}^2\big)$.

In equations **(5)** to **(10)** aerodynamic forces can be replaced by normal accelerations [7]. Transformation among wind axis aerodynamic forces and body axis forces are defined in terms of α and β.

$$\begin{bmatrix}\bar{X}\\ \bar{Y}\\ \bar{Z}\end{bmatrix} = \begin{bmatrix}-\cos\alpha\cos\beta & -\cos\alpha\sin\beta & \sin\alpha\\ -\sin\beta & \cos\beta & 0\\ -\sin\alpha\cos\beta & -\sin\alpha\sin\beta & -\cos\alpha\end{bmatrix}\begin{bmatrix}D\\ Y\\ L\end{bmatrix} \tag{14}$$

Normal accelerations are calculated from body axis forces.

$$a_x = \frac{\bar{X}+T}{m}\quad,\quad a_y = \frac{\bar{Y}}{m}\quad,\quad a_z = \frac{\bar{Z}}{m} \tag{15}$$

where

$a_x = A_{x_b} + g_{atm}\sin\theta$, $a_y = A_{y_b} - g_{atm}\sin\emptyset\cos\theta$ and $a_z = A_{z_b} - g_{atm}\cos\emptyset\cos\theta$.

Now, it is possible to represent the wind axis dynamic equations in terms of normal accelerations.

$$\dot{V}_T = a_x\cos\alpha\cos\beta + a_y\sin\beta + a_z\sin\alpha\cos\beta - g\sin\gamma \tag{16}$$

$$\dot{\alpha} = q - \tan\beta\,(p\cos\alpha + r\sin\alpha) - \frac{1}{V_T\cos\beta}(-a_x\sin\alpha + a_z\cos\alpha + g_{atm}\cos\gamma\cos\mu) \tag{17}$$

$$\dot{\beta} = -r\cos\alpha + p\sin\alpha - \frac{\sin\beta}{V_T}(a_x\cos\alpha + a_z\sin\alpha) + \frac{a_y}{V_T}\cos\beta + \frac{g_{atm}}{V_T}\cos\gamma\sin\mu \tag{18}$$

$$\dot{\gamma} = \frac{a_x}{V_T}(\sin\alpha\cos\mu + \cos\alpha\sin\beta\sin\mu) - \frac{a_y}{V_T}\cos\beta\sin\mu + \frac{a_z}{V_T}(-\cos\alpha\cos\mu + \sin\alpha\sin\beta\sin\mu) - \frac{g_{atm}}{V_T}\cos\gamma \tag{19}$$

DOI: 10.13009/EUCASS2017-228

$$\dot{\mu} = \frac{p\cos\alpha + r\sin\beta}{\cos\beta} + \frac{a_y}{V_T}\cos\beta\cos\mu\tan\gamma + (a_x\sin\alpha - a_z\cos\alpha)\frac{(\tan\gamma\sin\mu+\tan\beta)}{V_T} - (a_x\cos\alpha + a_z\sin\alpha)\frac{(\tan\gamma\cos\mu\sin\beta)}{V_T} - \frac{g_{atm}\cos\gamma\cos\mu\tan\beta}{V_T} \quad \textbf{(20)}$$

$$\dot{\chi} = \frac{a_x}{V_T}\frac{(\sin\mu\sin\alpha - \cos\alpha\cos\mu\sin\beta)}{\cos\gamma} + \frac{a_y}{V_T}\frac{\cos\beta\cos\mu}{\cos\gamma} - \frac{a_z}{V_T}\frac{(\cos\alpha\sin\mu+\sin\alpha\sin\beta\cos\mu)}{\cos\gamma} \quad \textbf{(21)}$$

3.1 Outer Loop - Slow Dynamic Inversion

Slow state dynamic equations represent the relationship among wind axis angles and angular rates. Equations (17), (18) and (20) can be represented in the matrix format.

$$\begin{bmatrix}\dot{\alpha}\\ \dot{\beta}\\ \dot{\mu}\end{bmatrix} = \begin{bmatrix}f_\alpha(V_T,\alpha,\beta,\mu,\gamma)\\ f_\beta(V_T,\alpha,\beta,\mu,\gamma)\\ f_\mu(V_T,\alpha,\beta,\mu,\gamma)\end{bmatrix} + \begin{bmatrix}-\tan\beta\cos\alpha & 1 & -\tan\beta\sin\alpha\\ \sin\alpha & 0 & -\cos\alpha\\ \cos\alpha/\cos\beta & 0 & \sin\alpha/\cos\beta\end{bmatrix}\begin{bmatrix}p\\ q\\ r\end{bmatrix} \quad \textbf{(22)}$$

where

$$f_\alpha(V_T,\alpha,\beta,\mu,\gamma) = -\frac{1}{V_T\cos\beta}(-a_x\sin\alpha + a_z\cos\alpha + g_{atm}\cos\gamma\cos\mu),$$

$$f_\beta(V_T,\alpha,\beta,\mu,\gamma) = -\frac{\sin\beta}{V_T}(a_x\cos\alpha + a_z\sin\alpha) + \frac{g_{atm}}{V_T}\cos\gamma\sin\mu,$$

$$f_\mu(V_T,\alpha,\beta,\mu,\gamma) = \frac{a_y}{V_T}\cos\beta\cos\mu\tan\gamma + (a_x\sin\alpha - a_z\cos\alpha)\frac{(\tan\gamma\sin\mu+\tan\beta)}{V_T} - (a_x\cos\alpha + a_z\sin\alpha)\frac{(\tan\gamma\cos\mu\sin\beta)}{V_T} - \frac{g_{atm}\cos\gamma\cos\mu\tan\beta}{V_T}.$$

Desired angular rates can be calculated using the dynamic inversion technique.

$$\begin{bmatrix}p_c\\ q_c\\ r_c\end{bmatrix} = \begin{bmatrix}-\tan\beta\cos\alpha & 1 & -\tan\beta\sin\alpha\\ \sin\alpha & 0 & -\cos\alpha\\ \cos\alpha/\cos\beta & 0 & \sin\alpha/\cos\beta\end{bmatrix}^{-1}\left(\begin{bmatrix}\dot{\alpha}_d\\ \dot{\beta}_d\\ \dot{\mu}_d\end{bmatrix} - \begin{bmatrix}f_\alpha(V_T,\alpha,\beta,\mu,\gamma)\\ f_\beta(V_T,\alpha,\beta,\mu,\gamma)\\ f_\mu(V_T,\alpha,\beta,\mu,\gamma)\end{bmatrix}\right) \quad \textbf{(23)}$$

Slow dynamics are invertible unless $\beta = \mp\pi/2$.

$\dot{\alpha}_d$, $\dot{\beta}_d$ and $\dot{\mu}_d$ are computed with proportional controllers with respect to pilot commands. Proportional gains $(w_\alpha, w_\beta, w_\mu)$ are generally set to 1 or 2 rad/s in the outer loop [1]. Block diagram of the outer loop dynamic inversion control is demonstrated in Figure 2.

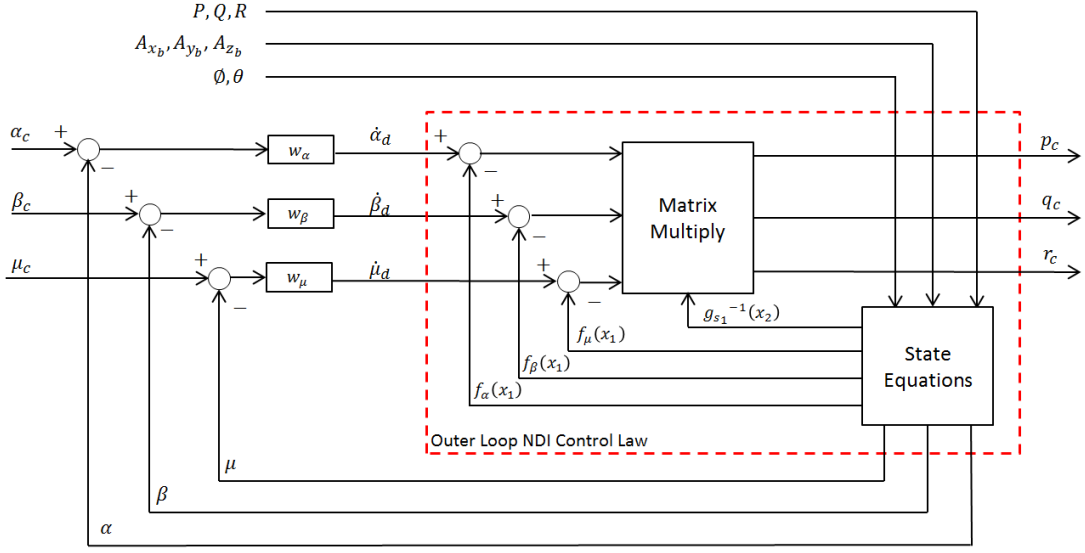

Figure 2: Outer loop slow dynamic inversion

DOI: 10.13009/EUCASS2017-228

3.2 Inner Loop - Fast Dynamic Inversion

Fast dynamic equations represent the relationship among the angular rates and the control surface deflections. Equations (11) to (13) can be represented in the matrix format by deriving the aerodynamic moments.

$$\begin{bmatrix}\dot{p}\\ \dot{q}\\ \dot{r}\end{bmatrix}=\begin{bmatrix}f_p(x_1)\\ f_q(x_1)\\ f_r(x_1)\end{bmatrix}+\begin{bmatrix}g_{p_{\delta_a}}(x_2) & 0 & g_{p_{\delta_r}}(x_2)\\ 0 & g_{q_{\delta_e}}(x_2) & 0\\ g_{r_{\delta_a}}(x_2) & 0 & g_{r_{\delta_r}}(x_2)\end{bmatrix}\begin{bmatrix}\delta_a\\ \delta_e\\ \delta_r\end{bmatrix} \quad \textbf{(24)}$$

where

$x_1=(V_T,\alpha,\beta,p,q,r,\delta_{LEF},\delta_e),\ x_2=(\alpha,\beta,\delta_e,\delta_{LEF},Q_c),$

$f_p(x_1)=c_1qr+c_2pq+c_3Q_cS\bar{b}\hat{l}+c_4Q_cS\bar{b}\hat{n}+c_4qh_{eng},$

$f_q(x_1)=c_5pr-c_6(p^2-r^2)+c_7Q_cS\bar{c}\hat{m}-c_7rh_{eng},$

$f_r(x_1)=c_8pq-c_2rq+c_4Q_cS\bar{b}\hat{l}+c_9Q_cS\bar{b}\hat{n}+c_9qh_{eng}$

with aerodynamic coefficients;

$\hat{l}=\delta_{C_{l_\beta}}(\alpha)\beta+\frac{p\bar{b}}{2V_T}\left\{C_{l_p}(\alpha)+\delta_{C_{l_{p_{LEF}}}}(\alpha)\left(1-(\delta_{LEF}/25)\right)\right\}+\frac{r\bar{b}}{2V_T}\left\{C_{l_r}(\alpha)+\delta_{C_{l_{r_{LEF}}}}(\alpha)\left(1-(\delta_{LEF}/25)\right)\right\}+C_l(\alpha,\beta,\delta_e)+\delta C_{l_{LEF}}\left(1-(\delta_{LEF}/25)\right)$

$\hat{m}=C_{M_T}-\hat{m}_{\delta_e}\,\delta_e$

$C_{M_T}=\delta_{C_m}(\alpha)+\frac{q\bar{c}}{2V_T}\left\{C_{m_q}(\alpha)+\delta_{C_{m_{q_{LEF}}}}(\alpha)\left(1-(\delta_{LEF}/25)\right)\right\}+\delta C_{m_{LEF}}\left(1-(\delta_{LEF}/25)\right)+C_{Z_T}(\alpha,\beta,q,\delta_e)\left(x_{cg_r}-x_{cg}\right)+\delta_{C_{m_{\delta s}}}(\alpha,\delta_e)+C_m(\alpha,\beta,\delta_e)$

$\hat{m}_{\delta_e}=\left(C_{M_T}(\alpha,\beta,q,\delta_e+0.1)-C_{M_T}(\alpha,\beta,q,\delta_e-0.1)\right)/\left(0.2(\pi/180)\right)$

$\hat{n}=\delta_{C_{n_\beta}}(\alpha)\beta+\frac{p\bar{b}}{2V_T}\left\{C_{n_p}(\alpha)+\delta_{C_{n_{p_{LEF}}}}(\alpha)\left(1-(\delta_{LEF}/25)\right)\right\}+\frac{r\bar{b}}{2V_T}\left\{C_{n_r}(\alpha)+\delta_{C_{n_{r_{LEF}}}}(\alpha)\left(1-(\delta_{LEF}/25)\right)\right\}+C_n(\alpha,\beta,\delta_e)+\delta C_{n_{LEF}}\left(1-(\delta_{LEF}/25)\right)$

and

$g_{p_{\delta_a}}(x_2)=\left(\left(\delta_{C_{l_{\delta_a}}}/21.5\right)c_3+\left(\delta_{C_{n_{\delta_a}}}/21.5\right)c_4\right)Q_cS\bar{b}$

$g_{p_{\delta_r}}(x_2)=\left(\left(\delta_{C_{l_{\delta_r}}}/30\right)c_3+\left(\delta_{C_{n_{\delta_r}}}/30\right)c_4\right)Q_cS\bar{b}$

$g_{q_{\delta_e}}(x_2)=Q_cS\bar{c}\hat{m}_{\delta_e}$

$g_{r_{\delta_a}}(x_2)=\left(\left(\delta_{C_{l_{\delta_a}}}/21.5\right)c_4+\left(\delta_{C_{n_{\delta_a}}}/21.5\right)c_9\right)Q_cS\bar{b}$

$g_{r_{\delta_r}}(x_2)=\left(\left(\delta_{C_{l_{\delta_r}}}/30\right)c_4+\left(\delta_{C_{n_{\delta_r}}}/30\right)c_9\right)Q_cS\bar{b}$

Desired control surface deflections are calculated by dynamic inversion technique.

$$\begin{bmatrix}{\delta_a}^d\\ {\delta_e}^d\\ {\delta_r}^d\end{bmatrix}=\begin{bmatrix}g_{p_{\delta_a}}(x_2) & 0 & g_{p_{\delta_r}}(x_2)\\ 0 & g_{q_{\delta_e}}(x_2) & 0\\ g_{r_{\delta_a}}(x_2) & 0 & g_{r_{\delta_r}}(x_2)\end{bmatrix}^{-1}\left(\begin{bmatrix}\dot{p}_d\\ \dot{q}_d\\ \dot{r}_d\end{bmatrix}-\begin{bmatrix}f_p(x_1)\\ f_q(x_1)\\ f_r(x_1)\end{bmatrix}\right) \quad \textbf{(25)}$$

$\dot{p}_d$, $\dot{q}_d$ and $\dot{r}_d$ are computed with proportional controllers with respect to outer loop angular rate commands. Proportional gains (w_p,w_q,w_r) are generally set to 5 or 10 rad/s in the inner loop [1]. Block diagram of inner loop dynamic inversion control is given in Figure 3.

DOI: 10.13009/EUCASS2017-228

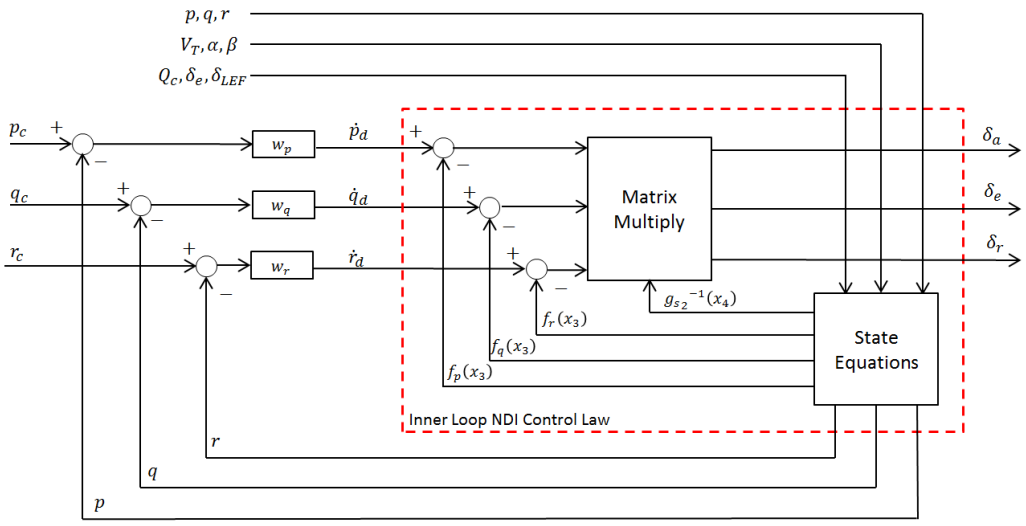

Figure 3: Inner loop fast dynamic inversion

In Figure 4, the resultant control law structure is shown as the combination of outer and inner loop controllers. The dash line indicates the virtual control loop which generates the necessary pilot command $\dot{\mu}_d$. In this control loop, a first order low-pass filter with a time constant of $0.25s$ is included in order to build a proper pilot signal.

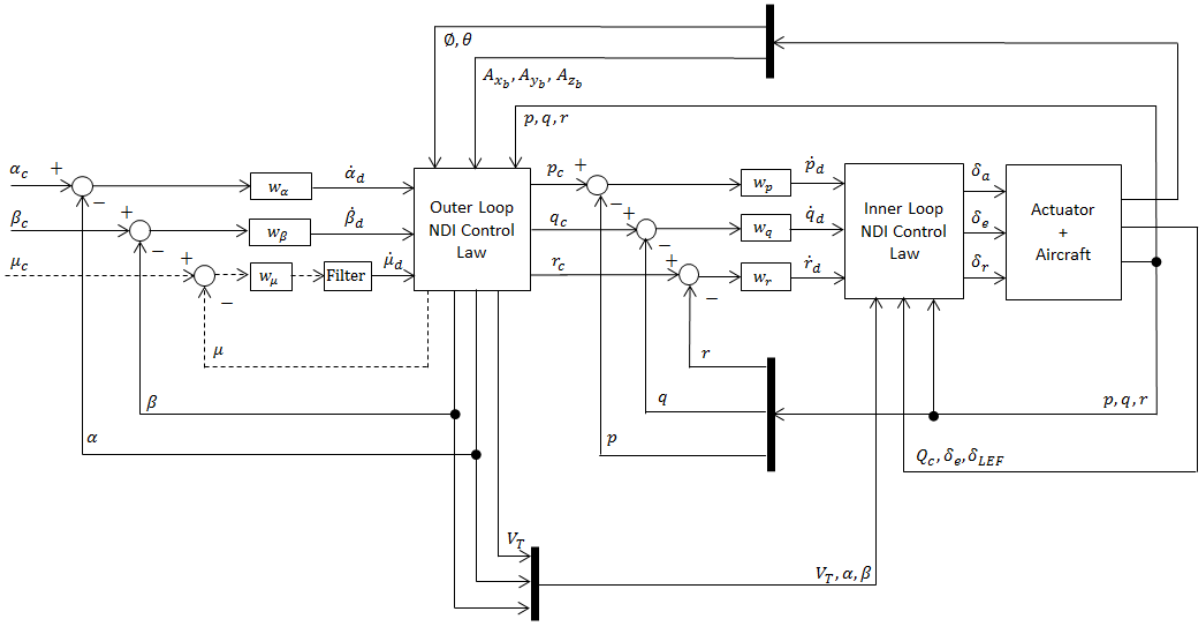

Figure 4: Nonlinear dynamic inversion control

4. Eigenstructure Assignment

Eigenstructure assignment is a linear control technique which places the closed loop poles into desired locations and for multi input systems, it also gives the designer a flexibility to manipulate the corresponding eigenvectors. For a linear time independent system with n states and m control inputs $(m < n)$, the designer can arbitrarily assign the m elements of the each eigenvector [8].

4.1 Longitudinal Linear Control Law Design

Longitudinal control law is based on the linearized short period dynamics of the aircraft. Linearized longitudinal state equations are derived in terms of small perturbations [6].

$$\begin{bmatrix}\Delta\dot{q}\\ \Delta\dot{\alpha}\end{bmatrix} = A_{lon}\begin{bmatrix}\Delta q\\ \Delta\alpha\end{bmatrix} + B_{lon}\Delta\delta_e \tag{26}$$

DOI: 10.13009/EUCASS2017-228

where

$\begin{bmatrix}\Delta q\\ \Delta\alpha\\ \Delta\delta_e\end{bmatrix} = \begin{bmatrix}q(t)-q^{eq}\\ \alpha(t)-\alpha^{eq}\\ \delta_e(t)-{\delta_e}^{eq}\end{bmatrix}$, $(.)^{eq}$ is the trim condition and $q^{eq}=0$.

An angle of attack command tracking system can be designed by including an additional error state $\left(\dot{\xi}_\alpha = \Delta\alpha^{ref} - \Delta\alpha\right)$.

$$\frac{d}{dt}\begin{bmatrix}\Delta q\\ \Delta\alpha\\ \xi_\alpha\end{bmatrix} = A_{lon}\begin{bmatrix}\Delta q\\ \Delta\alpha\\ \xi_\alpha\end{bmatrix} + B_{lon}\,\Delta\delta_e + \begin{bmatrix}0\\0\\1\end{bmatrix}\Delta\alpha^{ref} \quad \textbf{(27)}$$

If we assume that $\Delta\alpha^{ref}$ is a step input then the steady state system behaviour can be represented as shown in the equation below [9].

$$\frac{d}{dt}\begin{bmatrix}\Delta q(t)-\Delta q(\infty)\\ \Delta\alpha(t)-\Delta\alpha(\infty)\\ \xi_\alpha(t)-\xi_\alpha(\infty)\end{bmatrix} = A_{lon}\begin{bmatrix}\Delta q(t)-\Delta q(\infty)\\ \Delta\alpha(t)-\Delta\alpha(\infty)\\ \xi_\alpha(t)-\xi_\alpha(\infty)\end{bmatrix} + B_{lon}[\Delta\delta_e(t)-\Delta\delta_e(\infty)] \quad \textbf{(28)}$$

Since this is a single input system, an asymptotically stabilizing gain matrix K_α can be calculated using eigenvalue assignment technique. For $K_{lon} = [k_q \quad k_\alpha \quad -k_i]$ the block diagram of the control system is given in Figure 5.

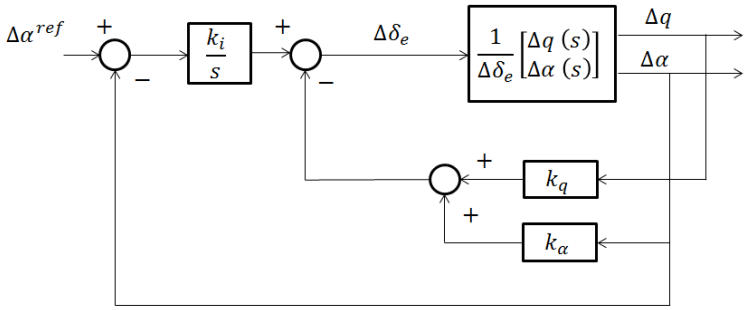

Figure 5: Longitudinal linear control system

Computation of the gain matrix is illustrated with an example. Longitudinal aircraft dynamics are linearized at a trim condition of 10kft and 200kts.

$$\begin{bmatrix}\Delta\dot{q}\\ \Delta\dot{\alpha}\\ \dot{\xi}_\alpha\end{bmatrix} = \begin{bmatrix}-0.772 & -1.012 & 0\\ 0.927 & -0.574 & 0\\ 0 & -1 & 0\end{bmatrix}\begin{bmatrix}\Delta q\\ \Delta\alpha\\ \xi_\alpha\end{bmatrix} + \begin{bmatrix}-3.635\\ -0.078\\ 0\end{bmatrix}\Delta\delta_e$$

Controllability matrix:

$C_o = \begin{bmatrix}-3.635 & 2.8852 & 1.1374\\ -0.078 & -3.325 & 4.583\\ 0 & 0.078 & 3.325\end{bmatrix}$, $rank(C_o) = 3 \Longrightarrow$ the system is controllable.

The system can be transformed into controller form by the similarity transformation matrix P.

$P = \begin{bmatrix}\ell\\ \ell A_{lon}\\ \ell {A_{lon}}^2\end{bmatrix} = \begin{bmatrix}-0.0001 & 0.0067 & 0.2916\\ 0.0063 & -0.2953 & 0\\ -0.2786 & 0.1631 & 0\end{bmatrix}$ where $\ell = {C_o}^{-1}(n,:)$ and $(n,:)$ denotes the n^{th} row.

The controller form of the linearized system can be computed as:

$A_c = PA_{lon}P^{-1} = \begin{bmatrix}0 & 1 & 0\\ 0 & 0 & 1\\ 0 & -1.3813 & -1.346\end{bmatrix}$ and $B_c = PB_{lon} = \begin{bmatrix}0\\0\\1\end{bmatrix}$.

A basis vector $[M_j \quad -D_j]^T$ of the controllable pair (A_{lon}, B_{lon}) for the closed loop system pole s_j satisfies:

DOI: 10.13009/EUCASS2017-228

$$\left[s_j I - A_{lon}, B_{lon}\right]\begin{bmatrix} M_j \\ -D_j \end{bmatrix} = 0 \tag{29}$$

where

$\begin{bmatrix} M_j \\ -D_j \end{bmatrix} = \begin{bmatrix} P^{-1}S(s_j) \\ -D(s_j) \end{bmatrix}$ and $D(s) \triangleq {B_m}^{-1}[\Lambda(s) - A_m \mathrm{S}(s)] = s^3 + s^2 1.346 + s\ 1.381$ with

$A_m = A_c(n,:) = [0 \quad -1.3813 \quad -1.346]$

$B_m = B_c(n,:) = 1$

$\Lambda(s) \triangleq s^n = s^3$

$\mathrm{S}(s) \triangleq [1 \quad s \quad \cdots \quad s^{n-1}]^n = [1 \quad s \quad s^2]^T$.

v_j is defined as the corresponding right eigenvector of the closed loop system pole s_j.

$$\left[s_j I - A_{lon}, B_{lon}\right]\begin{bmatrix} v_j \\ K_{lon} v_j \end{bmatrix} = 0 \tag{30}$$

For single input systems, the following equation is defined [10].

$$\begin{bmatrix} v_j \\ K_{lon} v_j \end{bmatrix} = \begin{bmatrix} M_j \\ -D_j \end{bmatrix} \tag{31}$$

where $K_{lon} = -WV^{-1}$, $W = [D_1 \quad D_2 \quad D_3]$ and $V = [v_1 \quad v_2 \quad v_3]$.

If the desired closed loop poles are selected as $s_{1,2} = -1.2 \pm 1.2j$ and $s_3 = -6$ then accordingly the basis vectors are calculated as following:

$\begin{bmatrix} M_1 \\ -D_1 \end{bmatrix} = \begin{bmatrix} 2.41 + j8.06 \\ 4.12 - j3.89 \\ 3.34 + j0.09 \\ -1.8 - j1.24 \end{bmatrix}$, $\begin{bmatrix} M_2 \\ -D_2 \end{bmatrix} = \begin{bmatrix} M_1 \\ -D_1 \end{bmatrix}^*$ and $\begin{bmatrix} M_3 \\ -D_3 \end{bmatrix} = \begin{bmatrix} -118.81 \\ 17.77 \\ 2.96 \\ 175.83 \end{bmatrix}$, $[.]^*$ refers to complex conjugate.

W and V matrices are calculated as following:

$W = [1.8 + j1.24 \quad 1.8 - j1.24 \quad -175.83]$ and $V = \begin{bmatrix} 2.41 + j8.06 & 2.41 - j8.06 & -118.81 \\ 4.12 - j3.89 & 4.12 + j3.89 & 17.77 \\ 3.34 + j0.09 & 3.34 - j0.09 & 2.96 \end{bmatrix}$

and finally the gain matrix is:

$K_{lon} = -WV^{-1} = [-1.867 \quad -3.428 \quad 5.038]$.

4.2 Lateral-Directional Linear Control Law Design

Lateral-directional control law is based on the linearized dutch-roll and roll-subsidence dynamics of the aircraft. Linearized lateral-directional state equations are derived in terms of small perturbations and transformed into stability axis state variables [6].

$$\frac{d}{dt}\begin{bmatrix} \Delta r_s \\ \Delta\beta \\ \Delta p_s \end{bmatrix} = A_{lat}\begin{bmatrix} \Delta r_s \\ \Delta\beta \\ \Delta p_s \end{bmatrix} + B_{lat}\begin{bmatrix} \Delta\delta_a \\ \Delta\delta_r \end{bmatrix} \tag{32}$$

where

$\begin{bmatrix} \Delta r_s \\ \Delta\beta \\ \Delta p_s \\ \Delta\delta_a \\ \Delta\delta_r \end{bmatrix} = \begin{bmatrix} r_s(t) - {r_s}^{eq} \\ \beta(t) - \beta^{eq} \\ p_s(t) - {p_s}^{eq} \\ \delta_a(t) - {\delta_a}^{eq} \\ \delta_r(t) - {\delta_r}^{eq} \end{bmatrix}$, $(.)^{eq}$ is the trim condition and ${r_s}^{eq} = \beta^{eq} = {p_s}^{eq} = 0$.

DOI: 10.13009/EUCASS2017-228

A stability axis roll rate and sideslip angle command tracking system can be designed by including the additional error states $\xi_{p_s} = \Delta {p_s}^{ref} - \Delta p_s$ and $\xi_\beta = \Delta \beta^{ref} - \Delta \beta$.

$$\frac{d}{dt}\begin{bmatrix} \Delta r_s \\ \Delta\beta \\ \Delta p_s \\ \xi_\beta \\ \xi_{p_s} \end{bmatrix} = A_{lat}\begin{bmatrix} \Delta r_s \\ \Delta\beta \\ \Delta p_s \\ \xi_\beta \\ \xi_{p_s} \end{bmatrix} + B_{lat}\begin{bmatrix} \Delta\delta_a \\ \Delta\delta_r \end{bmatrix} + \begin{bmatrix} 0 & 0 \\ 0 & 0 \\ 0 & 0 \\ 1 & 0 \\ 0 & 1 \end{bmatrix}\begin{bmatrix} \Delta\beta^{ref} \\ {\Delta p_s}^{ref} \end{bmatrix} \tag{33}$$

If we assume that $\Delta\beta^{ref}$ and ${\Delta p_s}^{ref}$ are step inputs then the steady state system behaviour can be represented as shown in the equation below [9].

$$\frac{d}{dt}\begin{bmatrix} \Delta r_s(t) - \Delta r_s(\infty) \\ \Delta\beta(t) - \Delta\beta(\infty) \\ \Delta p_s(t) - \Delta p_s(\infty) \\ \xi_\beta(t) - \xi_\beta(\infty) \\ \xi_{p_s}(t) - \xi_{p_s}(\infty) \end{bmatrix} = A_{lat}\begin{bmatrix} \Delta r_s(t) - \Delta r_s(\infty) \\ \Delta\beta(t) - \Delta\beta(\infty) \\ \Delta p_s(t) - \Delta p_s(\infty) \\ \xi_\beta(t) - \xi_\beta(\infty) \\ \xi_{p_s}(t) - \xi_{p_s}(\infty) \end{bmatrix} + B_{lat}\begin{bmatrix} \Delta\delta_a(t) - \Delta\delta_a(\infty) \\ \Delta\delta_r(t) - \Delta\delta_r(\infty) \end{bmatrix} + \begin{bmatrix} 0 & 0 \\ 0 & 0 \\ 0 & 0 \\ 1 & 0 \\ 0 & 1 \end{bmatrix}\begin{bmatrix} \Delta\beta^{ref}(t) - \Delta\beta^{ref}(\infty) \\ {\Delta p_s}^{ref}(t) - {\Delta p_s}^{ref}(\infty) \end{bmatrix} \tag{34}$$

Since this is a multi-input system, an asymptotically stabilizing gain matrix K_{lat} can be computed using eigenstructure assignment technique.

For $K_{lat} = \begin{bmatrix} k_{r_s} & k_\beta & k_{p_s} & -k_{i_\beta} & -k_{i_p} \end{bmatrix}$ the block diagram of the control system is given in Figure 6.

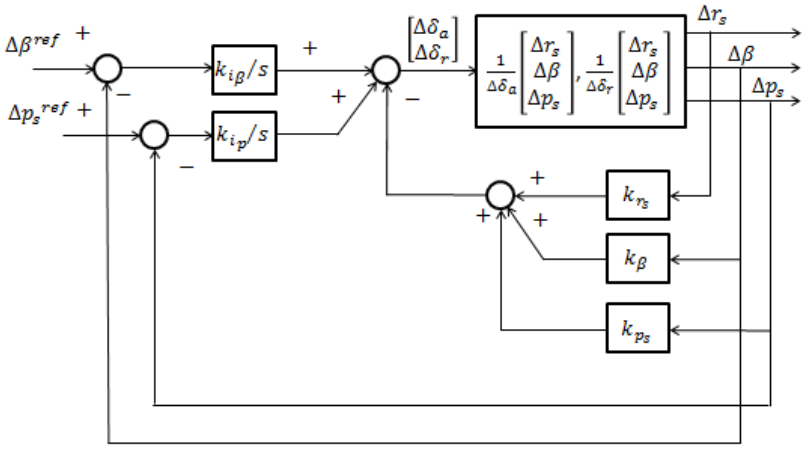

Figure 6: Lateral linear control system

Computation of the gain matrix is illustrated with an example. Lateral-directional aircraft dynamics are linearized at a trim condition of 10kft and 200kts.

$$\frac{d}{dt}\begin{bmatrix} \Delta r_s \\ \Delta\beta \\ \Delta p_s \\ \xi_\beta \\ \xi_{p_s} \end{bmatrix} = \begin{bmatrix} -0.383 & 4.88 & 0.172 & 0 & 0 \\ -0.994 & -0.147 & 0.0024 & 0 & 0 \\ 1.0017 & -13.84 & -1.476 & 0 & 0 \\ 0 & -1 & 0 & 0 & 0 \\ 0 & 0 & -1 & 0 & 0 \end{bmatrix}\begin{bmatrix} \Delta r_s \\ \Delta\beta \\ \Delta p_s \\ \xi_\beta \\ \xi_{p_s} \end{bmatrix} + \begin{bmatrix} 1.487 & -1.53 \\ 0.0074 & 0.021 \\ -12.01 & 2.1096 \\ 0 & 0 \\ 0 & 0 \end{bmatrix}\begin{bmatrix} \Delta\delta_a \\ \Delta\delta_r \end{bmatrix}$$

Controllability matrix:

$$C_o = \begin{bmatrix} b_1 & b_2 & Ab_1 & Ab_2 & A^2b_1 & \cdots \end{bmatrix} = \begin{bmatrix} 1.487 & -1.53 & -2.6 & 1.051 & -3.076 \\ 0.007 & 0.021 & -1.508 & 1.522 & 2.851 \\ -12.01 & 2.109 & 19.11 & -4.937 & -9.945 \cdots \\ 0 & 0 & -0.007 & -0.021 & 1.508 \\ 0 & 0 & 12.01 & -2.109 & -19.11 \end{bmatrix},$$

$rank(C_o) = 5 \Longrightarrow$ the system is controllable.

The system can be transformed into controller form by the similarity transformation matrix *P*. Matrix *P* can be constructed by the following steps:

DOI: 10.13009/EUCASS2017-228

Step 1: Reorder the first 5 linearly independent columns of C_o in the order of $[b_1 \quad A_{lat}b_1 \quad {A_{lat}}^2 b_1 \quad b_2 \quad A_{lat}b_2]$.

Step 2: Compute the inverse of the matrix $\bar{C_o}$ in Step 1.

Step 3: Determine controllability indices μ_1 & μ_2. ($\mu_1 = 3$ & $\mu_2 = 2$)

Step 4: Take the rows μ_1 and $\mu_1 + \mu_2$ in ${\bar{C_o}}^{-1}$ as ℓ_1 and ℓ_2.

Step 5: Construct the similarity transformation matrix as $P = [\ell_1 \quad \ell_1 A_{lat} \quad \ell_1 {A_{lat}}^2 \quad \ell_2 \quad \ell_2 A_{lat}]^T$.

The controller form of the linearized system can be computed as:

$$A_c = PA_{lat}P^{-1} = \begin{bmatrix} 0 & 1 & 0 & 0 & 0 \\ 0 & 0 & 1 & 0 & 0 \\ 0 & -5.254 & -1.846 & 0 & -1.074 \\ 0 & 0 & 0 & 0 & 1 \\ 0 & 3.733 & 0 & 0 & -0.16 \end{bmatrix} \text{ and } B_c = PB_{lat} = \begin{bmatrix} 0 & 0 \\ 0 & 0 \\ 1 & -1.018 \\ 0 & 0 \\ 0 & 1 \end{bmatrix}.$$

A basis vector $[M_j \quad -D_j]^T$ of the controllable pair (A_{lat}, B_{lat}) for the closed loop system pole s_j satisfies:

$$[s_j I - A_{lat}, B_{lat}] \begin{bmatrix} M_j \\ -D_j \end{bmatrix} = 0 \tag{35}$$

where

$$\begin{bmatrix} M_j \\ -D_j \end{bmatrix} = \begin{bmatrix} P^{-1}S(s_j) \\ -D(s_j) \end{bmatrix} \text{ and } D(s) \triangleq {B_m}^{-1}[\Lambda(s) - A_m \mathrm{S}(s)] = \begin{bmatrix} s^3 + s^2 1.846 + s\,1.454 & s^2 1.018 + s\,1.237 \\ 3.733s & s^2 + s\,0.1602 \end{bmatrix} \text{ with}$$

$$A_m = \begin{bmatrix} A_c(\mu_1, :) \\ A_c(\mu_1 + \mu_2, :) \end{bmatrix} = \begin{bmatrix} 0 & -5.254 & -1.846 & 0 & -1.074 \\ 0 & 3.733 & 0 & 0 & -0.16 \end{bmatrix}$$

$$B_m = \begin{bmatrix} B_c(\mu_1, :) \\ B_c(\mu_1 + \mu_2, :) \end{bmatrix} = \begin{bmatrix} 1 & -1.018 \\ 0 & 1 \end{bmatrix} \quad ; (\mu_1, :) \text{ denotes the } {\mu_1}^{th} \text{ row e.g.}$$

$$\Lambda(s) \triangleq \begin{bmatrix} s^{\mu_1} & 0 \\ 0 & s^{\mu_2} \end{bmatrix} = \begin{bmatrix} s^3 & 0 \\ 0 & s^2 \end{bmatrix},$$

$$\mathrm{S}(s) \triangleq \begin{bmatrix} 1 & s & \cdots & s^{\mu_1 - 1} & 0 & 0 & \cdots & 0 \\ 0 & 0 & \cdots & 0 & 1 & s & \cdots & s^{\mu_2 - 1} \end{bmatrix}^T = \begin{bmatrix} 1 & s & s^2 & 0 & 0 \\ 0 & 0 & 0 & 1 & s \end{bmatrix}^T.$$

v_j is defined as the corresponding right eigenvector of the closed loop system pole s_j.

$$[s_j I - A_{lat}, B_{lat}] \begin{bmatrix} v_j \\ K_{lat} v_j \end{bmatrix} = 0 \tag{36}$$

For multi input systems, the following equation is defined [10]:

$$\begin{bmatrix} v_j \\ K_{lat} v_j \end{bmatrix} = \begin{bmatrix} M_j \\ -D_j \end{bmatrix} a_j \text{ , } a_j \in \mathbb{C}^{mx1}. \tag{37}$$

where;

$K_{lat} = -WV^{-1}$, $W = [D_1 a_1 \quad D_2 a_2 \quad D_3 a_3 \quad D_4 a_4 \quad D_5 a_5]$ and $V = [v_1 \quad v_2 \quad v_3 \quad v_4 \quad v_5]$.

If the desired closed loop poles are selected as $s_{1,2} = -0.9 \pm 0.9j$, $s_3 = -4.5$, $s_4 = -5.5$ and $s_5 = -6.5$ then accordingly the basis vectors are calculated as following:

$$\begin{bmatrix} M_1 \\ -D_1 \end{bmatrix} = \begin{bmatrix} -0.13 - j2.28 & 0.01 - j0.01 \\ 1.34 - j1.36 & -0.03 + j0.03 \\ 2.75 + j16.7 & 9.11 - j9.11 \\ 1.5 + j0.01 & -0.03 \\ -7.75 + j10.8 & 10.12 \\ 0.15 - j0.22 & -1.11 - j0.54 \\ 3.36 - j3.36 & -0.14 - j1.48 \end{bmatrix}, \begin{bmatrix} M_2 \\ -D_2 \end{bmatrix} = \begin{bmatrix} M_1 \\ -D_1 \end{bmatrix}^*, \begin{bmatrix} M_3 \\ -D_3 \end{bmatrix} = \begin{bmatrix} 29.46 & 0.07 \\ 6.87 & -0.13 \\ -229.46 & 45.53 \\ 1.53 & -0.03 \\ -51 & 10.12 \\ -60.3 & 15.05 \\ 16.8 & 19.53 \end{bmatrix}$$

DOI: 10.13009/EUCASS2017-228

$\begin{bmatrix} M_4 \\ -D_4 \end{bmatrix} = \begin{bmatrix} 44.18 & 0.09 \\ 8.44 & -0.16 \\ -346.5 & 55.65 \\ 1.54 & -0.03 \\ -63 & 10.12 \\ -118.54 & 24 \\ 20.53 & 29.37 \end{bmatrix}$ and $\begin{bmatrix} M_5 \\ -D_5 \end{bmatrix} = \begin{bmatrix} 61.88 & 0.01 \\ 10.03 & -0.19 \\ -487.57 & 65.77 \\ 1.54 & -0.03 \\ -75 & 10.12 \\ -206.1 & 34.97 \\ 24.27 & 41.21 \end{bmatrix}$, $[.]^*$ refers to complex conjugate.

Since the system has two control inputs, the designer can arbitrarily assign the two elements of each eigenvector. Hence, the dutch-roll and roll-subsidence modes can be decoupled by eliminating the cross coupled terms in eigenvectors [11].

$$\begin{matrix} \Delta r_s \rightarrow \\ \Delta \beta \rightarrow \\ \Delta p_s \rightarrow \\ \xi_\beta \rightarrow \\ \xi_{p_s} \rightarrow \end{matrix} \underbrace{\begin{bmatrix} x \\ x \\ 0 \\ x \\ 0 \end{bmatrix}}_{v_1} \underbrace{\begin{bmatrix} x \\ x \\ 0 \\ x \\ 0 \end{bmatrix}}_{v_2 = v_1^*} \underbrace{\begin{bmatrix} 0 \\ 0 \\ x \\ x \\ x \end{bmatrix}}_{v_3} \underbrace{\begin{bmatrix} x \\ x \\ 0 \\ x \\ 0 \end{bmatrix}}_{v_4} \underbrace{\begin{bmatrix} 0 \\ 0 \\ x \\ x \\ x \end{bmatrix}}_{v_5}$$

Proposed eigenvector structure can be achieved by the appropriate selection of a_j vectors. An appropriate selection might be achieved by the inverse solution of the problem.

$$a_1 = \begin{bmatrix} M_1(3,:) \\ M_1(5,:) \end{bmatrix}^{-1} \begin{bmatrix} 10^{-10} \\ 10^{-10} \end{bmatrix}, a_2 = {a_1}^*, \quad a_3 = \begin{bmatrix} M_3(1,:) \\ M_3(2,:) \end{bmatrix}^{-1} \begin{bmatrix} 10^{-4} \\ 10^{-4} \end{bmatrix}, \quad a_4 = \begin{bmatrix} M_4(3,:) \\ M_4(5,:) \end{bmatrix}^{-1} \begin{bmatrix} 10^{-10} \\ 10^{-10} \end{bmatrix}$$

$$a_5 = \begin{bmatrix} M_5(1,:) \\ M_5(2,:) \end{bmatrix}^{-1} \begin{bmatrix} 10^{-4} \\ 10^{-4} \end{bmatrix}.$$

The resultant eigenvector satisfies the desired structure.

$$V = [M_1 a_1 \quad M_2 a_2 \quad M_3 a_3 \quad M_4 a_4 \quad M_5 a_5] = \begin{bmatrix} 0.52 - j0.99 & 0.52 + j0.99 & 0 & 6.19 & 0 \\ 0.9 - j0.2 & 0.9 + j0.2 & 0 & 1.03 & 0 \\ 0 & 0 & -0.025 & 0 & -0.028 \\ 0.61 + j0.38 & 0.61 - j0.38 & 0 & 0.187 & 0 \\ 0 & 0 & -0.0056 & 0 & -0.004 \end{bmatrix}$$

The gain matrix K_{lat} assigns the closed loop poles to desired locations and also builds the decoupling eigenvector structure.

$$K_{lat} = -WV^{-1} = \begin{bmatrix} -1.0183 & 2.1932 & -0.9738 & -1.2361 & 2.9239 \\ -5.3226 & 5.9256 & -1.0292 & -7.0369 & 2.7808 \end{bmatrix}$$

DOI: 10.13009/EUCASS2017-228

5. Simulation Results

Proposed control strategies in section 3 and 4 were subjected to a supermanoeuvrability test. A super-manoeuvre can be defined as a rapid and simultaneous pitch-up and roll motion. Three triangular form pitch-up motions of 20°, 30°and 40° angle of attack has been aimed with a synchronized roll motion of 120° bank angle. Simulations were initialized with the 10kft pressure altitude and 200kts airspeed trim condition. Engine power has not been changed during the simulations. Linear controllers were scheduled with respect to airspeed and altitude in order to adapt the changing flight conditions.

In Figure 7, results of 20° angle of attack manoeuvre are presented. Both linear and nonlinear controllers were able to perform the manoeuvre since this is a pre-stall region. However, the sideslip motion could not have been eliminated by the linear controller.

30° angle of attack manoeuvre results are demonstrated in Figure 8. Results show that the linear controller is still able to perform the manoeuvre but the tracking performance becomes unsatisfactory. In addition the aileron and rudder control surface deflections were saturated; therefore the proper control of sideslip angle could not have been achieved.

In Figure 9, it can be seen that the linear controller is not able to control the aircraft at 40°angle of attack. Nonlinear controller on the other hand can still conduct the manoeuvre as expected.

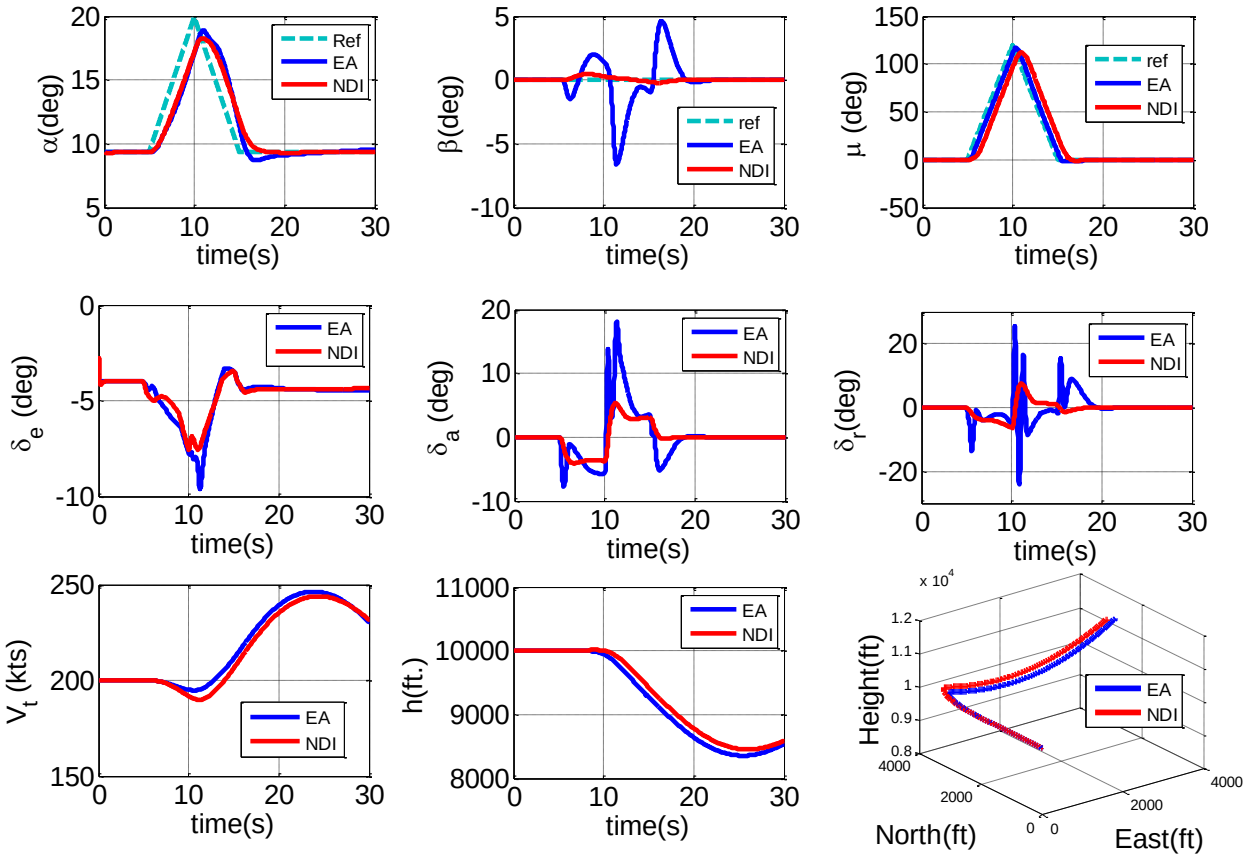

Figure 7: **20**° angle of attack manoeuvre

DOI: 10.13009/EUCASS2017-228

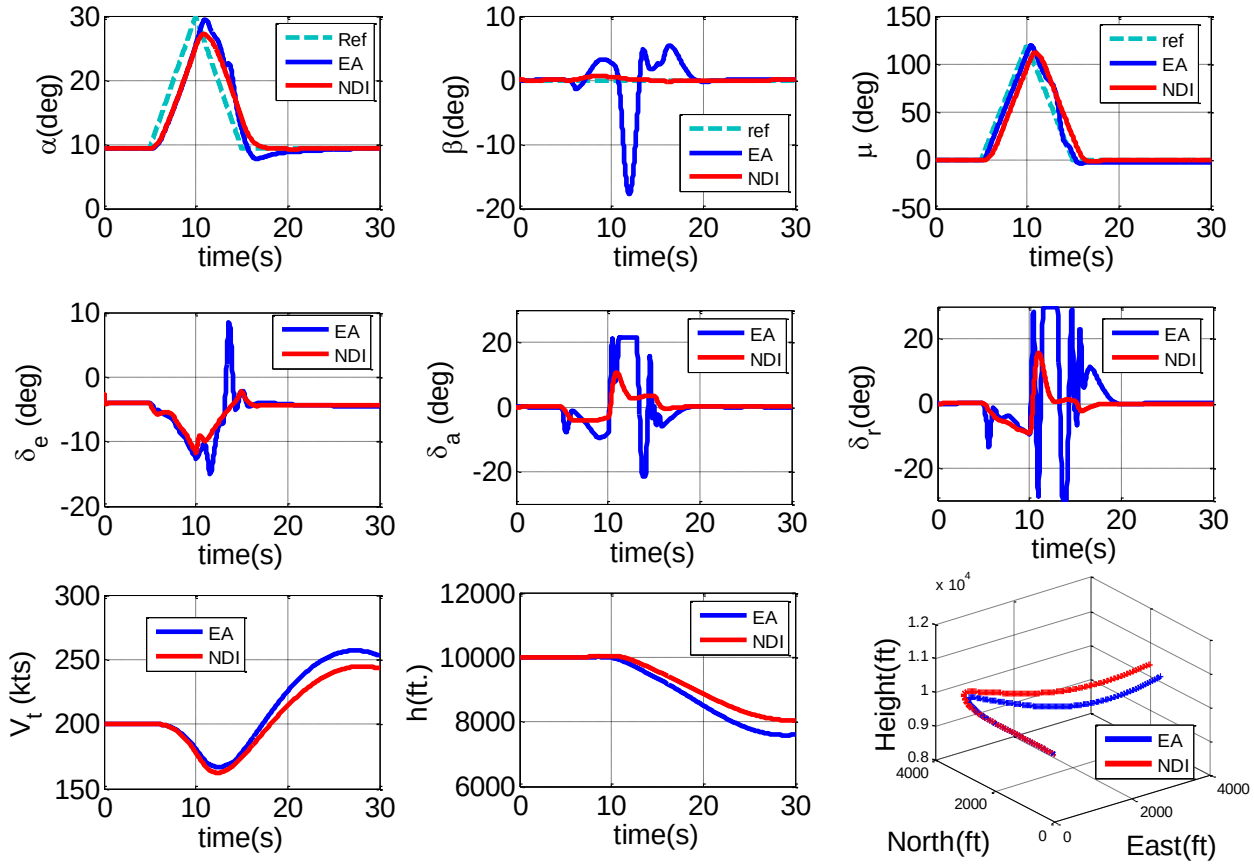

Figure 8: **30**° angle of attack manoeuvre

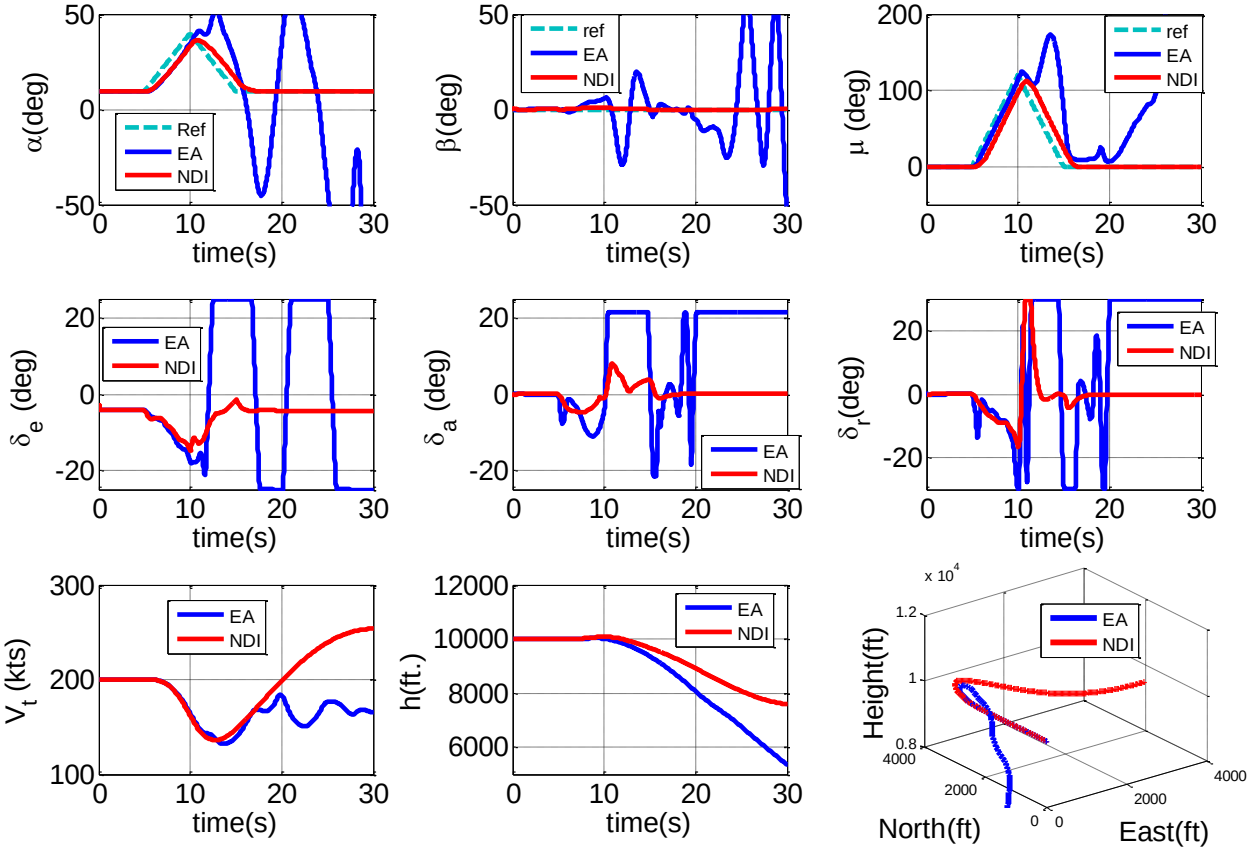

Figure 9: **40**° angle of attack manoeuvre

DOI: 10.13009/EUCASS2017-228

6. Conclusion

Control methods for high angle of attack manoeuvring problem have been investigated. Nonlinear dynamic inversion and eigenstructure assignment design techniques were applied on nonlinear F-16 aircraft dynamics. Nonlinear dynamic inversion control law was designed in two steps. The first step is the inversion of slow dynamics; the second step is the inversion of fast dynamics. Inversion of the fast dynamics was based on the aerodynamic database of F-16 aircraft. Eigenstructure assignment is a linear multi input control technique. However the longitudinal motion of F-16 simulation model is controlled by the elevator only, therefore the longitudinal control design reduced to an eigenvalue assignment problem. Lateral-directional motion is controlled by the aileron and rudder, so it was possible to apply eigenstructure assignment technique. Eigenvalues of the closed loop lateral-directional control system were placed in the desired locations furthermore the structure of the corresponding eigenvectors was shaped in order to decouple the dutch-roll and roll-subsisdence modes.
A high angle of attack manoeuvre was simulated in Simulink by using the proposed control strategies and then the simulation results were provided in a comparative fashion. Results show that as the angle of attack increases, the eigenstructure assignment technique begins to fail, because it does not address the coupling problem of the longitudinal and lateral dynamics of the aircraft. Nonlinear dynamic inversion shows great superiority at high angle of attack regions, in addition the control power usage is more effective than the eigenstructure assignment.

7. Acknowledgements

Special thanks to Aircraft Group at Turkish Aerospace Industries, Inc. for the support they have shown during the preparation of this study.

References

[1] Snell, A., F. Enns, and W. Garrard Jr. 1992. Nonlinear Inversion Flight Control for a Supermaneuverable *Aircraft. Journal of Guidance, Control and Dynamics*. Vol 15, No. 4.
[2] Nguyen, T., E. Ogburn, P. Gilbert, S. Kibler, W. Brown, and L. Deal. 1979. Simulator Study of Stall/Post-Stall Characteristics of a Fighter Airplane with Relaxed Longitudinal Static Stability. Technical Paper 1538. National Aeronautics and Space Administration.
[3] Sonneveldt, L., 2010. Nonlinear F-16 Model Description. Delft University of Technology.
[4] Huo, Y., Model of F-16 Fighter Aircraft. University of Southern California.
[5] De Marco, A., L. Duke, and S. Berndt. 2007. A General Solution to the Aircraft Trim Problem. *AIAA Modeling and Simulation Technologies Conference and Exhibit.*2007-6703.
[6] Stengel, R. 2004. Flight Dynamics. Princeton University.
[7] Chen, H.B., and S.G. Zhang. 2008. Robust Dynamic Inversion Flight Control Law. IEEE 1-4244-2386.
[8] Andry Jr., A.N., Shapiro, E.Y., and J.C. Chung. 1983. Eigenstructure Assignment for Linear Systems. IEEE 0018-9251.
[9] Ogata, K. 2010. Modern Control Engineering 5th Edition. Prentice Hall.
[10] Antsaklis, J.P. and A.N., Michel. 2007. A Linear Systems Primer. University of Notr Dame.
[11] Sobel, M.K., and E.Y. Shapiro. 1987. Application of Eigenstructure Assignment to Flight Control Design: Some Extensions. Journal of Guidance Vol.10, No.1.